

Journal Pre-proofs

Bioactive bisbenzylisoquinoline alkaloids from the roots of *Stephania tetrandra*

Renzhong Wang, Yanfei Liu, Guoru Shi, Jie Zhou, Jiayuan Li, Li Li, Jiqiao Yuan, Xuyu Li, Dequan Yu

PII: S0045-2068(19)32035-8
DOI: <https://doi.org/10.1016/j.bioorg.2020.103697>
Reference: YBIOO 103697

To appear in: *Bioorganic Chemistry*

Received Date: 27 November 2019
Revised Date: 19 February 2020
Accepted Date: 23 February 2020

Please cite this article as: R. Wang, Y. Liu, G. Shi, J. Zhou, J. Li, L. Li, J. Yuan, X. Li, D. Yu, Bioactive bisbenzylisoquinoline alkaloids from the roots of *Stephania tetrandra*, *Bioorganic Chemistry* (2020), doi: <https://doi.org/10.1016/j.bioorg.2020.103697>

This is a PDF file of an article that has undergone enhancements after acceptance, such as the addition of a cover page and metadata, and formatting for readability, but it is not yet the definitive version of record. This version will undergo additional copyediting, typesetting and review before it is published in its final form, but we are providing this version to give early visibility of the article. Please note that, during the production process, errors may be discovered which could affect the content, and all legal disclaimers that apply to the journal pertain.

© 2020 Published by Elsevier Inc.



Bioactive bisbenzylisoquinoline alkaloids from the roots of *Stephania tetrandra*

Renzhong Wang, Yanfei Liu, Guoru Shi, Jie Zhou, Jiayuan Li, Li Li, Jiqiao Yuan,
Xuyu Li and Dequan Yu *

*State Key Laboratory of Bioactive Substance and Function of Natural Medicines,
Institute of Materia Medica, Chinese Academy of Medical Sciences and Peking Union
Medical College, Beijing 100050, People's Republic of China*

***Corresponding Author**

E-mail: dqyu@imm.ac.cn (D. Yu). Tel: +86-10-63165224. Fax: +86-10-63017757.

ABSTRACT: Ten new bisbenzylisoquinoline alkaloids (**1-10**) and eight known analogues (**11-18**) were obtained from the roots of *Stephania tetrandra*. The structures of these compounds were determined by spectroscopic methods, single-crystal X-ray diffraction, electronic circular dichroism analyses, and chemical method. Compounds **1**, **15**, and **16** showed the better anti-inflammatory activities with IC_{50} values of 15.26 ± 2.99 , 6.12 ± 0.25 , and 5.92 ± 1.89 μ M, respectively. Compound **18** possessed cytotoxic activities against MCF-7, HCT-116, and HepG2 cell lines with IC_{50} values of 2.81 ± 0.06 , 3.66 ± 0.26 , and 2.85 ± 0.15 μ M, respectively.

Keywords: *Stephania tetrandra*; Menispermaceae; Bisbenzylisoquinoline alkaloids; Anti-inflammatory activities; Cytotoxicity

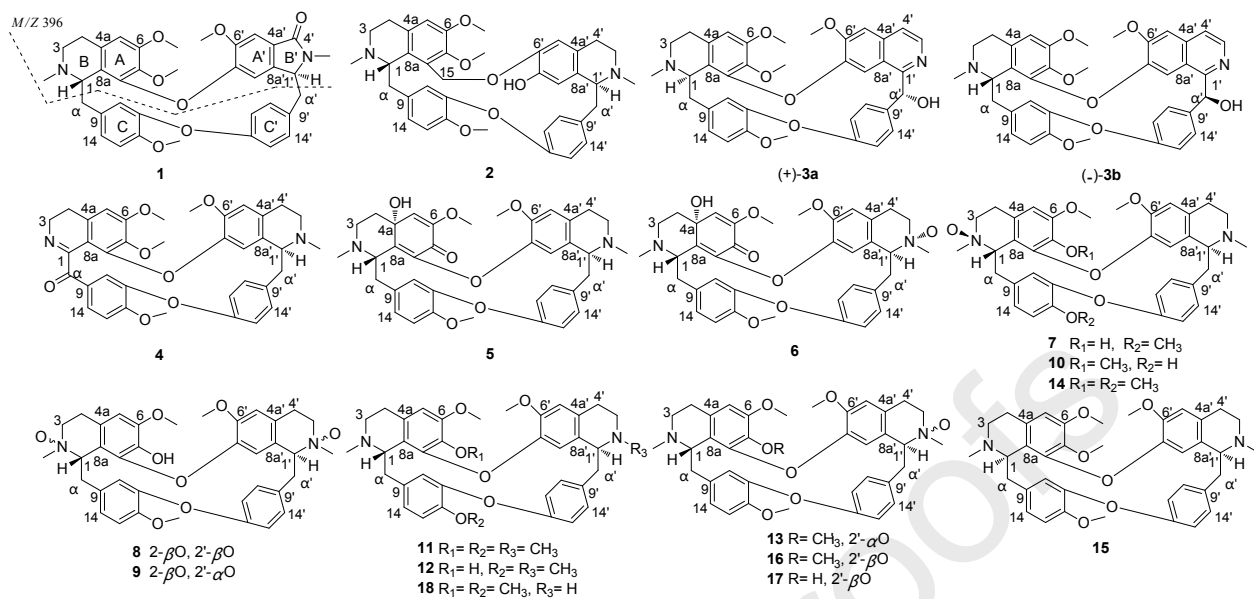


Fig. 1. The structures for compounds 1-18

1. Introduction

Bisbenzylisoquinoline alkaloids are structurally diverse and fascinating alkaloid class, which consist of two benzylisoquinoline units linked by diphenyl ether, benzyl phenyl ether or biphenyl bonds [1]. To date, nearly 500 bisbenzylisoquinoline alkaloids have been isolated and structurally characterized from the plants which mostly distribute the families of Berberidaceae, Menispermaceae, Monimiaceae, and Ranunculaceae [1,2]. Some of these bisbenzylisoquinoline alkaloids possess various biological activities, such as antiplasmodial, anti-inflammatory, antibacterial, antifungal, cytotoxic, and antioxidant activities [3-6]. *Stephania tetrandra* S. Moore is a commonly used herb, belonging to the Menispermaceae family. Its roots, named “Fen Fang Ji” in Chinese, have been used for treatments of rheumatism, dropsy, dysuria, and eczema [7]. Previous chemical work showed that *S. tetrandra* afforded a series of bisbenzylisoquinoline alkaloids [8-10]. Among these, tetrandrine (**11**) is the main components, which has been reported to exhibit wide pharmacological activities [11], such as anti-inflammatory and anticancer.

In order to discover structurally diverse bisbenzylisoquinoline alkaloids with anti-inflammatory and cytotoxic activities, a detailed chemical investigation on the roots of *S. tetrandra* was carried out. In the present study, 18 bisbenzylisoquinoline alkaloids were successfully isolated, including ten new bisbenzylisoquinoline alkaloids (**1-10**) and eight known compounds (**11-18**) (Fig. 1). The known compounds were identified as tetrandrine (**11**) [12], fangchinoline (**12**) [13,14], tetrandrine 2'-*N*- α -oxide (**13**) [15,16], fenfangjine A (**14**) [8], isotetrandrine (**15**) [17], tetrandrine

2'-*N*- β -oxide (**16**) [18], fenfangjine C (**17**) [8], and cycleanorine (**18**) [19] by comparison their physical and spectroscopic data with literature values. The isolated compounds **1-18** were examined for anti-inflammatory activity and cytotoxicity. Herein, the details of isolation, structure elucidation and biological evaluation of these compounds are presented.

2. Materials and methods

2.1. General experimental procedures

The UV spectra, optical rotations, and ECD spectra were measured with JASCO V-650, JASCO P-2000, and JASCO J-815 spectrometers, respectively. Melting points were recorded on an XT5B microscope melting point apparatus. IR spectra were measured by a Nicolet 5700 spectrometer (FT-IR microscope transmission). The NMR spectra were acquired by Mercury-400 and Bruker AVIIIHD 600 MHz spectrometers. HRESIMS/MS data were obtained using Dionex UltiMate 3000 UHPLC equipped with Thermo Scientific Q Exactive Focus Mass spectrometer. The X-ray crystallographic data were obtained from an Agilent Xcalibur Eos Gemini diffractometer with Cu-K α radiation ($\lambda = 1.5418\text{\AA}$). Analytical HPLC was performed on an Agilent 1260 infinity system equipped with a DAD-UV detector. Preparative HPLC was conducted on a Shimadzu LC-6AD liquid chromatography system equipped with a SPD-20A UV detector and an ODS column (C18, 250 \times 10mm, 5 μ m, CAPCELL PAK-MG II, Kyoto, Japan).

2.2. Plant material

The roots of *Stephania tetrandra* were collected from Ruichang, Jiangxi Province, China, in December 2017, and were authenticated by Professor Lin Ma, Institute of Materia Medica, Chinese Academy of Medical Sciences and Peking Union Medical College. A voucher specimen (ID-S-2937) was preserved in the herbarium of Institute of Materia Medica, Chinese Academy of Medical Sciences and Peking Union Medical College.

2.3. Extraction and isolation

The dried and powdered roots of *Stephania tetrandra* (98 kg) were extracted with 95% EtOH under reflux (100 L × 3). The solution was evaporated under reduced pressure and the residue (8.0 kg) was then added into 1% HCl solution with vigorous stirring. The acidic solution was filtered, and the acidic filtrate was then basified with concentrated NH₄OH to produce free alkaloids and exhaustively extracted with CHCl₃ to give a crude alkaloid mixture (2.1 kg), which was subjected to a silica gel column using gradient elution with petroleum ether-acetone and CHCl₃-MeOH (1:0 to 25:1 and 30:1 to 0:1) to afford seven fractions (A-G). Fraction A (1.3 kg) was recrystallized in acetone to give **11** (1.2 kg), and the acetone solution was evaporated and the residue (100 g) was chromatographed further on silica gel eluting with CHCl₃-MeOH gradient system (1:0 to 0:1) to afford six fractions (A1-A6). Fraction A3 (34.2 g) was applied to column chromatography over silica gel eluting with petroleum ether-CH₂Cl₂ and CH₂Cl₂-MeOH gradient system (5:1 and 30:1 to 0:1) to afford five fractions (A3a-A3e). Fraction A3d (29.2 g) was separated by repeated chromatography, including silica gel column chromatography

(EtOAc/MeOH/NH₄OH gradient), Sephadex LH-20 (CH₂Cl₂/MeOH, 1:1) or MPLC (ODS, MeCN/H₂O, 30:70 to 100:0, NH₄OH, 0.01%), and was further purified by preparative HPLC to afford **1** (7.0 mg, MeCN/H₂O, 55:45, NH₄OH, 0.01%), **2** (12.0 mg, MeCN/H₂O, 65:35, NH₄OH, 0.01%), and **3** (7.3 mg, MeCN/H₂O, 56:44, NH₄OH, 0.01%). Compound **3** was subjected to chiral HPLC using a CHIRALPAK AD-H column (n-hexane/isopropyl alcohol, 82:18) to afford (+)-**3a** (3.5 mg) and (–)-**3b** (1.3 mg). Fraction A3e (1.6 g) was applied to MPLC (ODS, MeCN/H₂O, 30:70 to 100:0, NH₄OH, 0.01%) to obtain six fractions (A3e1-A3e6). A3e1 (100 mg), A3e3 (30 mg), and A3e4 (50 mg) were purified by preparative HPLC (MeCN/H₂O, 37:63, NH₄OH, 0.01%) to give **13** (8.2 mg), **14** (5.1 mg), and **16** (13.0 mg), respectively. Fraction A4 (40.0 g) was fractionated by silica gel column chromatography using gradient elution with EtOAc-MeOH (20:1 to 0:1) to afford four fractions (A4a-A4d). Fraction A4c was crystallized in MeOH to give **12** (1.0 g). Fraction A4d (8.0 g) was chromatographed using Sephadex LH-20 (CH₂Cl₂/MeOH, 1:1), MPLC (ODS, MeCN/H₂O, 30:70 to 100:0, NH₄OH, 0.01%), and preparative HPLC to yield **4** (4.8 mg, MeCN/H₂O, 48:52, diethylamine, 0.01%) and **15** (12.3 mg, MeCN/H₂O, 64:36, diethylamine, 0.01%). Fraction B (400g) was recrystallized in EtOH, and the EtOH solution was evaporated to give the residue (129 g), which was performed on a silica gel column chromatography eluting with CH₂Cl₂-MeOH and EtOAc-MeOH-NH₄OH gradient system (20:1 to 10:1 and 20:2:1 to 10:2:1) to afford eight fractions (B1-B8). After purification by Sephadex LH-20 (CH₂Cl₂/MeOH, 1:1), fraction B6 (3.2 g) was applied to MPLC (ODS, MeCN/H₂O, 5:95 to 100:0, diethylamine, 0.01%) to give

seven fractions (B6a-B6f). Fraction B6a (40.0 mg) was purified by preparative HPLC (MeCN/H₂O, 18:82, diethylamine, 0.01%) to give **8** (9.2 mg) and **9** (5.0 mg). Preparative HPLC was used to purify compounds **7** (19.2 mg) and **17** (14.8 mg) from B6d (MeCN/H₂O, 28:72, diethylamine, 0.01%) and B6f (MeCN/H₂O, 37:63, diethylamine, 0.01%). Fraction B6b (63.2 mg) was chromatographed using MPLC (ODS, MeCN/H₂O, 24:76 to 30:70, diethylamine, 0.01%) and preparative HPLC to afford **6** (8.1 mg, MeCN/H₂O, 28:72, diethylamine, 0.01%) and **10** (6.0 mg, MeOH/H₂O, 60:40, diethylamine, 0.01%). Fraction B5 (13.4 g) was separated on Sephadex LH-20 (CH₂Cl₂/MeOH, 1:1), silica gel column (CH₂Cl₂/MeOH, 10:1, EtOAc/MeOH/NH₄OH, 20:2:1), MPLC (ODS, MeCN/H₂O, 30:70 to 100:0, diethylamine, 0.01%), and preparative HPLC to give **5** (30.0 mg, MeCN/H₂O, 43:57, diethylamine, 0.01%) and **18** (9.5 mg, MeCN/H₂O, 63:37, diethylamine, 0.01%).

2.3.1. Fenfangjine J (**1**)

colorless crystals (MeOH); mp 260-261°C; $[\alpha]_{\text{D}}^{20} +186$ (*c* 0.35, MeOH); UV (MeOH) λ_{max} (log ϵ) 207 (4.56), 267 (3.37), 293 (3.48) nm; IR ν_{max} 3445, 2933, 1679, 1582, 1580, 1299, 1122, 828 cm⁻¹; ECD (MeOH) λ_{max} ($\Delta\epsilon$) 233 (+57.26), 264.5 (-9.28), 290.5 (-4.87) nm; ¹H and ¹³C NMR (CDCl₃) data see Tables 1 and 2; HRESIMS *m/z* 623.2754 [M+H]⁺ (calcd for C₃₇H₃₉O₈N₂, 623.2752).

2.3.2. Fenfangjine K (**2**)

colorless crystals (MeOH); mp 252-253°C; $[\alpha]_{\text{D}}^{20} -2$ (*c* 0.55, CHCl₃); UV (MeOH) λ_{max} (log ϵ) 207 (4.42), 287.4 (3.41) nm; IR ν_{max} 3547, 2937, 1600, 1507, 1269, 1230, 1126, 1005 cm⁻¹; ECD (MeOH) λ_{max} ($\Delta\epsilon$) 216.5 (+26.65), 240 (+14.80), 291.5 (+1.46)

nm; ^1H and ^{13}C NMR (CDCl_3) data see Tables 1 and 2; HRESIMS m/z 623.3117 $[\text{M}+\text{H}]^+$ (calcd for $\text{C}_{38}\text{H}_{43}\text{O}_6\text{N}_2$, 623.3116).

2.3.3. (\pm)-Fenfangjine L (**3**)

white amorphous powder; $[\alpha]_{\text{D}}^{20}$ +73 (c 0.40, MeOH); UV (MeOH) λ_{max} ($\log \epsilon$) 204 (4.24), 238 (4.25), 311 (2.99), 325 (3.03) nm; IR ν_{max} 3339, 2934, 1606, 1504, 1265, 1227, 862 cm^{-1} ; ^1H and ^{13}C NMR (CDCl_3) data see Tables 1 and 2; HRESIMS m/z 621.2596 $[\text{M}+\text{H}]^+$ (calcd for $\text{C}_{37}\text{H}_{37}\text{O}_7\text{N}_2$, 621.2595); (+)-Fenfangjine L (**3a**): $[\alpha]_{\text{D}}^{20}$ +80 (c 0.35, MeOH); ECD (MeOH) λ_{max} ($\Delta\epsilon$) 240.5 (+21.20), 293 (−0.31), 322.5 (+1.43) nm. (−)-Fenfangjine L (**3b**): $[\alpha]_{\text{D}}^{20}$ −76 (c 0.13, MeOH); ECD (MeOH) λ_{max} ($\Delta\epsilon$) 241 (−15.33), 291.5 (+1.28), 322 (−0.59) nm.

2.3.4. Fenfangjine M (**4**)

white amorphous powder; $[\alpha]_{\text{D}}^{20}$ +222 (c 0.32, CHCl_3); UV (MeOH) λ_{max} ($\log \epsilon$) 204 (4.31), 227 (4.09), 288.8 (3.64) nm; IR ν_{max} 3413, 2939, 1678, 1600, 1506, 1267, 1120, 1016 cm^{-1} ; ECD (MeOH) λ_{max} ($\Delta\epsilon$) 216 (−2.23), 233 (+24.72), 264.5 (+2.67), 305 (−1.31), 337 (+2.51) nm; ^1H and ^{13}C NMR (CDCl_3) data see Tables 1 and 2; HRESIMS m/z 621.2593 $[\text{M}+\text{H}]^+$ (calcd for $\text{C}_{37}\text{H}_{37}\text{O}_7\text{N}_2$, 621.2595).

2.3.5. Fenfangjine N (**5**)

white amorphous powder; $[\alpha]_{\text{D}}^{20}$ +327 (c 1.9, CHCl_3); UV (MeOH) λ_{max} ($\log \epsilon$) 205.6 (4.86), 237.8 (4.35), 274.4 (3.98) nm; IR ν_{max} 3396, 2930, 1674, 1509, 1286, 1226, 1108, 838 cm^{-1} ; ECD (MeOH) λ_{max} ($\Delta\epsilon$) 216 (+70.76), 239 (−13.49), 256 (+13.31), 287 (+24.94) nm; ^1H and ^{13}C NMR (CDCl_3) data see Tables 1 and 2; HRESIMS m/z 625.2902 $[\text{M}+\text{H}]^+$ (calcd for $\text{C}_{37}\text{H}_{41}\text{O}_7\text{N}_2$, 625.2908).

2.3.6. Fenfangjine O (6)

white amorphous powder; $[\alpha]_{\text{D}}^{20}$ +244 (c 0.44, CHCl_3); UV (MeOH) λ_{max} ($\log \epsilon$) 205.2 (4.24), 237 (3.76), 274.4 (3.44) nm; IR ν_{max} 3374, 2938, 1669, 1510, 1284, 1260, 1113, 842 cm^{-1} ; ECD (MeOH) λ_{max} ($\Delta\epsilon$) 219 (+24.80), 240.5 (-3.02), 257.5 (+3.42), 287.5 (+8.19) nm; ^1H and ^{13}C NMR (CDCl_3) data see Tables 3 and 4; HRESIMS m/z 641.2854 $[\text{M}+\text{H}]^+$ (calcd for $\text{C}_{37}\text{H}_{41}\text{O}_8\text{N}_2$, 641.2857).

2.3.7. Fenfangjine P (7)

white amorphous powder; $[\alpha]_{\text{D}}^{20}$ +222 (c 1.0, CHCl_3); UV (MeOH) λ_{max} ($\log \epsilon$) 206 (4.13), 285.4 (3.14) nm; IR ν_{max} 3395, 2966, 1513, 1461, 1263, 1235, 1129, 881 cm^{-1} ; ECD (MeOH) λ_{max} ($\Delta\epsilon$) 220 (+100.90), 280.5 (+5.66) nm; ^1H and ^{13}C NMR (CDCl_3) data see Tables 3 and 4; HRESIMS m/z 625.2907 $[\text{M}+\text{H}]^+$ (calcd for $\text{C}_{37}\text{H}_{41}\text{O}_7\text{N}_2$, 625.2908).

2.3.8. Fenfangjine Q (8)

white amorphous powder; $[\alpha]_{\text{D}}^{20}$ +289 (c 0.57, CHCl_3); UV (MeOH) λ_{max} ($\log \epsilon$) 207.4 (4.53), 286.6 (3.43) nm; IR ν_{max} 3388, 2960, 1510, 1460, 1264, 1237, 1128 cm^{-1} ; ECD (MeOH) λ_{max} ($\Delta\epsilon$) 221 (+75.43), 275 (+4.02) nm; ^1H and ^{13}C NMR (CDCl_3) data see Tables 3 and 4; HRESIMS m/z 641.2858 $[\text{M}+\text{H}]^+$ (calcd for $\text{C}_{37}\text{H}_{40}\text{O}_8\text{N}_2$, 641.2857).

2.3.9. Fenfangjine R (9)

white amorphous powder; $[\alpha]_{\text{D}}^{20}$ +199 (c 0.35, CHCl_3); UV (MeOH) λ_{max} ($\log \epsilon$) 206.6 (4.49), 287 (3.29) nm; IR ν_{max} 3385, 2965, 1511, 1462, 1265, 1235, 1128 cm^{-1} ; ECD (MeOH) λ_{max} ($\Delta\epsilon$) 221 (+89.32), 285 (+4.93) nm; ^1H and ^{13}C NMR (CDCl_3) data

see Tables 3 and 4; HRESIMS m/z 641.2856 $[M+H]^+$ (calcd for $C_{37}H_{41}O_8N_2$, 641.2857).

2.3.10 Fenfangjine S (**10**)

white amorphous powder; $[\alpha]_D^{20}$ +268 (c 0.1, $CHCl_3$); UV (MeOH) λ_{max} ($\log \epsilon$) 207 (4.52), 286.2 (3.33) nm; IR ν_{max} 3406, 2934, 1503, 1454, 1261, 1122, 905 cm^{-1} ; ECD (MeOH) λ_{max} ($\Delta\epsilon$) 225 (+86.44), 272.5 (+6.09) nm; 1H and ^{13}C NMR ($CDCl_3$) data see Tables 3 and 4; HRESIMS m/z 625.2907 $[M+H]^+$ (calcd for $C_{37}H_{41}O_7N_2$, 625.2908).

2.4. Reduction of compounds **7**, **8**, and **9**

Compound **7** (15.8 mg) was dissolved in 10% HCl (30 ml), and then zinc powder (100 mg) was added. After being stirred at room temperature for 2 h, the mixture was adjusted to pH 9 with NH_4OH and then was extracted with CH_2Cl_2 (3 \times 30 ml). The CH_2Cl_2 layer was purified by preparative HPLC (MeCN/ H_2O , 58:42, diethylamine, 0.01%) to yield fangchinoline (**12**). Based on the same method, the reduction of compounds **8** and **9** also yielded fangchinoline (**12**).

2.5. X-ray crystallographic analysis of compounds **1**, **2**, and **12**.

Single crystals of **1**, **2**, and **12** were obtained from MeOH. The crystal data were collected on an Agilent Xcalibur Eos Gemini diffractometer using Cu-K α radiation (λ = 1.5418 Å). The crystal structures were solved by direct methods using the SHELXS-97 program and refined by the full-matrix least-squares difference Fourier method. Crystallographic data of **1**, **2**, and **12** have been deposited at the Cambridge Crystallographic Data Center (CCDC No. 1954074, 1954075, and 1954076

respectively) and can be obtained free of charge from the CCDC Web site (www.ccdc.cam.ac.uk).

2.5.1. Crystal data of **1**

$C_{37}H_{38}N_2O_7$, $M = 622.69$, orthorhombic, $a = 7.20673(16) \text{ \AA}$, $b = 11.8067(5) \text{ \AA}$, $c = 37.8914(8) \text{ \AA}$, $U = 3224.10(16) \text{ \AA}^3$, $T = 110.35(10)$, space group $P2_12_12_1$ (no. 19), $Z = 4$, $\mu(\text{Cu K}\alpha) = 0.723$, 11350 reflections measured, 6112 unique ($R_{\text{int}} = 0.0258$). The final $wR(F_2)$ was 0.0867 (all data). The goodness of fit and flack parameters were 1.032 and $-0.01(7)$, respectively.

2.5.2. Crystal data of **2**

$C_{38}H_{42}N_2O_6$, $M = 622.73$, orthorhombic, $a = 13.2047(3) \text{ \AA}$, $b = 13.8202(3) \text{ \AA}$, $c = 17.9059(4) \text{ \AA}$, $U = 3267.69(11) \text{ \AA}^3$, $T = 115.15(10)$, space group $P2_12_12_1$ (no. 19), $Z = 4$, $\mu(\text{Cu K}\alpha) = 0.687$, 11755 reflections measured, 6183 unique ($R_{\text{int}} = 0.0312$). The final $wR(F_2)$ was 0.1051 (all data). The goodness of fit and flack parameters were 1.055 and 0.00(10), respectively.

2.5.3. Crystal data of **12**

$C_{37}H_{40}N_2O_6$, $M = 608.71$, orthorhombic, $a = 7.26130(13) \text{ \AA}$, $b = 10.5190(2) \text{ \AA}$, $c = 39.8162(7) \text{ \AA}$, $U = 3041.22(10) \text{ \AA}^3$, $T = 109.95(10)$, space group $P2_12_12_1$ (no. 19), $Z = 4$, $\mu(\text{Cu K}\alpha) = 0.726$, 10594 reflections measured, 5732 unique ($R_{\text{int}} = 0.0240$). The final $wR(F_2)$ was 0.0949 (all data). The goodness of fit and flack parameters were 1.057 and 0.10(15), respectively.

2.6. ECD calculation

Conformational analysis was performed by the MOE software package using the MMFF94s molecular mechanics force field. The conformers with Boltzmann distribution of over 1% were chosen for ECD calculations. The chosen conformers were optimized at the WB97XD/6-31g(d) level using the Gaussian 09 program. The theoretical calculation of ECD was conducted using TDDFT methodology at the APFD/6-31g(d) level in MeOH. The ECD spectra were simulated by SpecDis and the final ECD spectra were obtained according to the Boltzmann distribution theory.

2.7. Anti-inflammatory activity assay

Peritoneal macrophages were obtained from C57BL/6 mice 3 days after intraperitoneal injection with 1.2 ml of 4% sterile thioglycolate. Then, cells were inoculated into 96-well plates (2×10^5 cells/well) containing RPMI 1640 medium with 5% fetal bovine serum and were cultured for 2 h under a humidified atmosphere with 5% CO₂ at 37 °C. The culture medium was replaced by fresh medium containing compounds (10^{-5} M). After incubation for 2h, the macrophages were then incubated with 1 µg/ml of LPS for 24h. The culture supernatants of macrophages were collected and Griess reagents were added into supernatants to determine the NO level. The absorbance was measured at 570 nm with a microplate reader. Dexamethasone (DEX) was used as a positive control.

2.8. Cytotoxicity assay

The five human cancer cells (A549, CMF-7, HCT-116, HepG2, and Capan 2) were cultured in the RPMI1640 medium containing 10% fetal bovine serum and 100 U/mL penicillin under a humidified atmosphere with 5% CO₂ at 37 °C . Cells were

plated into 96-well plates in 100 μL of medium and incubated for 24 h. The medium was replaced with fresh medium containing the tested compounds at concentrations of 0.1, 1, and 10 μM , respectively, which were carried out in triplicate. After 72 h, the mediums were replaced with 100 μL of MTT (0.5 mg/ml in medium), and the cells were incubated for 4 h. 200 μL of DMSO was then added and the absorbance was measured at 570 nm with a microplate reader. The inhibition rate was calculated by the following formula: $1 - \text{mean OD}_{\text{treated well}} / \text{mean OD}_{\text{blank well}}$. Paclitaxel was used as the positive control.

3. Results and discussion

Compound **1** was obtained as colorless crystals. Its molecular formula was determined to be $\text{C}_{37}\text{H}_{38}\text{O}_8\text{N}_2$ by the HRESIMS ion at m/z 623.2754 $[\text{M}+\text{H}]^+$ (calcd for $\text{C}_{37}\text{H}_{39}\text{O}_8\text{N}_2$, 623.2752), indicating 20 degrees of unsaturation. The IR spectrum suggested the presence of carbonyl (1679 cm^{-1}) and aromatic ring (1582 and 1508 cm^{-1}) functionalities. The ^1H NMR spectrum (Table 1) of **1** in the lower field showed the presence of a para-disubstituted benzene ring at δ_{H} 6.50 (1H, dd, $J = 8.4, 2.4$ Hz, H-10'), 6.79 (1H, dd, $J = 8.4, 2.4$ Hz, H-11'), 7.09 (1H, dd, $J = 8.4, 2.4$ Hz, H-13'), 7.29 (1H, dd, $J = 8.4, 2.4$ Hz, H-14'), a 1,3,4-trisubstituted benzene ring at δ_{H} 6.47 (1H, d, $J = 1.8$ Hz, H-10), 6.86 (1H, d, $J = 8.4$ Hz, H-13), 6.89 (1H, dd, $J = 8.4, 1.8$ Hz, H-14), and three aromatic singlet protons at δ_{H} 6.35 (1H, s, H-5), 7.21 (1H, s, H-5'), 6.40 (1H, s, H-8'). Six heteroatom-bearing singlet methyls [δ_{H} 3.78 (s, 6-OMe); 3.23 (s, 7-OMe); 3.91 (s, 12-OMe); 3.48 (s, 6'-OMe); 2.32 (s, 2-N-Me); 3.29 (s, 2'-N-Me)] were observed in the higher field. Analysis of the ^{13}C NMR spectrum

(Table 2) revealed the presence of 37 carbon signals, including the signals corresponding to the aforementioned units, four methylenes (δ_c 44.3, C-3; 22.3, C-4; 41.6, C- α ; 37.2, C- α'), two methines (δ_c 61.6, C-1; 61.2, C-1'), a carbonyl (δ_c 168.6, C-4') and 14 aromatic quaternary carbons. Further analysis of the ^1H and ^{13}C NMR data of **1** showed a similarity to those of tetrandrine (**11**) [12], except for the signals of B'-ring in **1**.

In the HMBC spectrum (Fig. 2), the HMBC correlations from H-5' to C-4', C-4a', and C-8a', from H-8' to C-1', C-4a', and C-8a', from 2'-N-CH₃ (δ_{H} 3.28) to C-1' and C-4', from H-1' to C-4', C-4a', and C-8a' constructed the B'-ring unit. The locations of all methoxy groups were corroborated by the ROESY correlations (Fig. 3) of OCH₃-6 (δ_{H} 3.77) with H-5, OCH₃-12 (δ_{H} 3.91) with H-13, and OCH₃-6' (δ_{H} 3.48) with H-5'. The MS/MS data of compound **1** displaying a fragment ion peak at m/z 396 (Fig.S5, Supporting Information) corresponded to the upper half of the molecule, due to the cleavage of double benzylic bonds. Thus, compound **1** was confirmed as a head-to-head bisbenzyl-isoquinoline alkaloid [20,21] that contains two diphenyl ether bridges occurring at C-8/C-7' and C-11/C-12'. The 2D structure of **1** was assigned as shown (Fig. 2). Fortunately, the crystals were obtained from methanol and the absolute configuration of **1** was determined as 1*S*, 1'*S* by single-crystal X-ray diffraction (Cu-K α) analysis (Fig. 4) with a Flack parameter of -0.01(7). Therefore, the structure of compound **1** was designated as fenfangjine J.

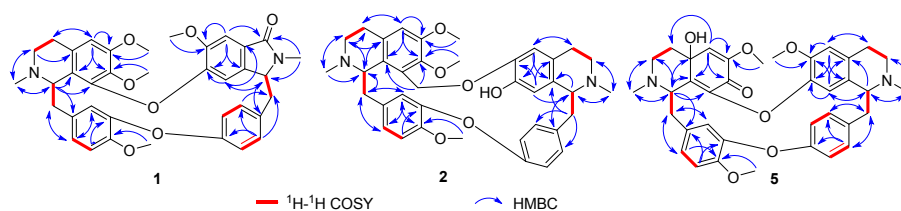


Fig. 2. Key ^1H - ^1H COSY and HMBC correlations of compounds **1**, **2**, and **5**

Compound **2**, colorless crystal, was assigned a molecular formula of $\text{C}_{38}\text{H}_{42}\text{O}_6\text{N}_2$ based on its HRESIMS peak at m/z 623.3117 $[\text{M}+\text{H}]^+$ (calcd for $\text{C}_{38}\text{H}_{43}\text{O}_6\text{N}_2$, 623.3116), implying 19 degrees of unsaturation. The UV spectrum (λ_{max} 207 and 287 nm) was very close to those of **11**, which indicated the presence of benzylisoquinoline moieties. Its IR spectrum showed the presence of hydroxy group (3547 cm^{-1}) and aromatic ring (1600 and 1507 cm^{-1}) functionalities. The ^{13}C NMR data (Table 2) of **2** were similar to those of **11** [12], except for a methylene at δ_{C} 62.1. However, the ^1H NMR spectrum (Table 1) of **2** in the lower field displayed only seven aromatic protons at room temperature. The three aromatic protons of C'-ring not be observed. The variable-temperature (50°C) 400 MHz ^1H NMR spectrum was carried out, which showed ten aromatic protons [δ_{H} 6.95 (1H, dd, $J = 8.4, 1.6$ Hz, H-14); 6.88 (1H, d, $J = 8.4$ Hz, H-13); 6.28 (1H, d, $J = 1.6$ Hz, H-10); 6.74 (1H, s, H-5); 7.10 (2H, brs, H-10'/14'); 6.70 (2H, brd, H-11'/13'); 6.49 (1H, s, H-5'); 6.48 (1H, s, H-8')]. Compared with **11** [12], the ^1H NMR spectrum of **2** revealed the presence of an additional methylene group [δ_{H} 5.10 (1H, d, $J = 9.2$ Hz, H-15a), 4.73 (1H, d, $J = 9.2$ Hz, H-15b)] and the absence of a methoxy group. The HMBC correlations from H-15 to C-7, C-8 and C-8a, from H-5 to C-6, C-7 and C-8a confirmed that the methylene (δ_{C} 62.1, C-15) was connected to the C-8 position of the A-ring. Comprehensive analysis of

^1H - ^1H COSY, HSQC and HMBC data (Fig. 2) demonstrated the presence of the two benzylisoquinoline moieties. The ROESY correlation (Fig. 3) of H₂-15 with H-5' confirmed that the methylene (δ_{C} 62.1, C-15) also was attached at C-6' via an ether bond. In addition, the MS/MS data of **2** showed a fragment ion peak at m/z 388 (Fig. S17, Supporting Information). These data indicated that **2** was the head-head connection. Therefore, compound **2** was identified to be an unusual bisbenzylisoquinoline alkaloid with C-15/6' benzyl phenyl ether bridge and C-11/12' diphenyl ether bridge and named fengfangjine K. The structure of **2** was confirmed by single-crystal X-ray diffraction analysis (Fig. 4), which also allowed assignment of the absolute configuration of **2** as 1*S*, 1'*S* [Flack parameter 0.00 (10)].

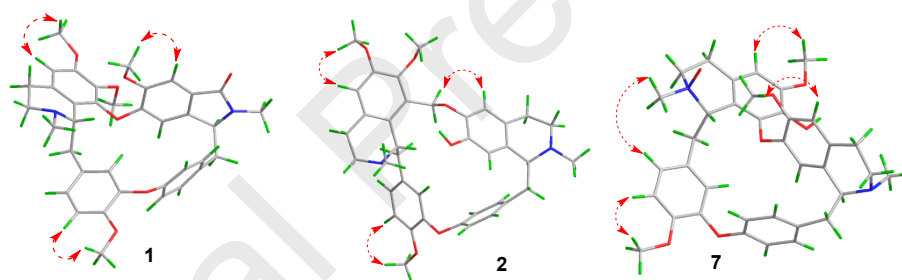


Fig. 3. Key ROESY correlations of compounds **1**, **2**, and **7**.

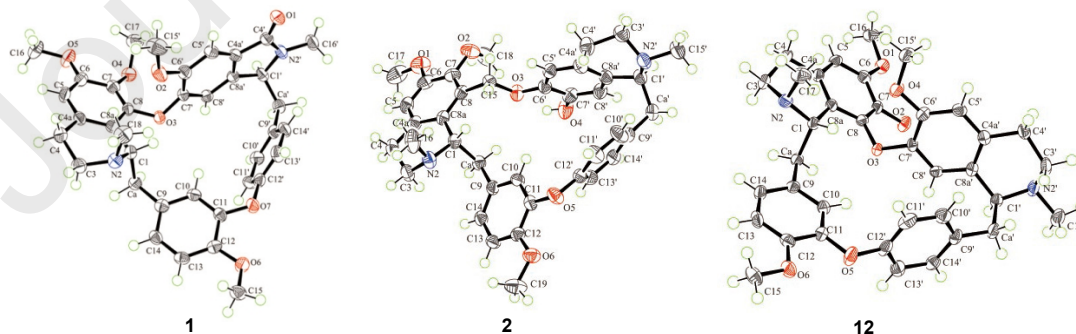


Fig. 4. X-ray ORTEP drawing of compounds **1**, **2**, and **12**.

Compound **3** was isolated as a white amorphous powder, which was found to have a molecular formula of $C_{37}H_{36}O_7N_2$ according to its HRESIMS peak at m/z 621.2596 $[M+H]^+$ (calcd for $C_{37}H_{37}O_7N_2$, 621.2595), with 21 degrees of unsaturation. The NMR features (Tables 1 and 2) of **3** were similar to those of **11** [12], except for the signals of B- or B'-ring. The 1H NMR spectrum (Table 1) of **3** revealed the presence of additional three protons [δ_H 8.37 (1H, d, $J = 5.4$ Hz), 7.50 (1H, d, $J = 5.4$ Hz), and 6.08 (1H, s)] in the lower field. While, only one $N-CH_3$ (δ_H 2.50) group was observed in the higher field. The ^{13}C NMR data (Table 2) combined with HSQC data indicated the presence of two aromatic methines (δ_C 138.4, 120.0), a downfield chemical shifted aromatic quaternary carbon (δ_C 157.4), and a oxygenated methine (δ_C 72.8). All of the data indicated that B- or B'-ring in **3** was an aromatic ring. The HMBC correlations from H-4' to C-3', C-5', and C-8a', from H-3' to C-4', C-4a', and C-1', from H-8' to C-1', C-4a', and from H- α' to C-1', C-9', C-10', and C-14' confirmed that the B'-ring in **3** was a pyridine ring and the hydroxyl group was present at C- α' . In addition, other $^1H-^1H$ COSY, HMBC, ROESY, and HRESIMS/MS data established the 2D structure of **3**. In the MS/MS spectrum of **3**, a weak fragment ion peak at m/z 379 (Fig. S30, Supporting Information) corresponded to the upper half of the molecule, which confirmed that compound **3** was a head-head bisbenzylisoquinoline with C-8/C-7' and C-11/C-12' diphenyl ether bridges. Compound **3** was analysed by chiral HPLC using an AD-H column, which afforded the enantiomers (+)-**3a** and (-)-**3b** with an ee value of approximately 34% for (+)-**3a** (Fig. S37, Supporting Information). Finally, the absolute configurations of (+)-**3a** and (-)-**3b** were

established as $1R, \alpha'R$ and $1S, \alpha'S$ by comparing the experimental and calculated ECD spectra (Fig. 5). Compounds (+)-**3a** and (-)-**3b** were assigned the names (+)-fenfangjine L and (-)-fenfangjine L, respectively.

Compound **4** was obtained as a white amorphous powder and possessed the same molecular ($C_{37}H_{36}O_7N_2$) as **3** based on the HRESIMS data (m/z 621.2593 $[M+H]^+$, calcd for $C_{37}H_{37}O_7N_2$, 621.2595). The IR spectrum revealed the presence of carbonyl (1678 cm^{-1}) functionality. The UV spectrum (λ_{max} 204, 227, and 288.8 nm) was same as those of cheratamine [22]. Comparison of the ^1H NMR data of **4** (Table 1) and cheratamine revealed a high degree of similarity. The difference mainly resided in the presence of the methoxy group (δ_{H} 3.96) in **4**. The HMBC correlation from OCH_3 -12 (δ_{H} 3.96) to C-12 revealed that the methoxy group was attached at C-12. In addition, the ROESY correlation of OCH_3 -12 (δ_{H} 3.96) with H-13 confirmed the location of methoxy group (δ_{H} 3.96). The MS/MS data of **4** showed a fragment ion peak at m/z 380 (Fig. S42, Supporting Information), corresponding to the upper half of the molecule. The positive optical rotation value and ECD cotton effects of **4** were similar to those of cheratamine [22], which indicated the absolute configuration of **4** was $1'S$. Thus, compound **4** was elucidated as fenfangjine M.

Compound **5**, white amorphous powder, had a molecular formula of $C_{37}H_{40}O_7N_2$ based on the HRESIMS ion at m/z 625.2902 $[M+H]^+$ (calcd for $C_{37}H_{41}O_7N_2$, 625.2908), indicating 19 degrees of unsaturation. The IR spectrum displayed absorption bands for hydroxy group (3396 cm^{-1}) and carbonyl (1674 cm^{-1}) functionalities. Analysis of the ^1H NMR data (Table 1) of **5** showed a

1,3,4-trisubstituted benzene ring at δ_{H} 6.68 (1H, d, $J = 1.8$ Hz, H-10), 6.87 (1H, d, $J = 8.4$ Hz, H-13), 6.84 (1H, dd, $J = 8.4, 1.8$ Hz, H-14), a para-disubstituted benzene ring at δ_{H} 6.33 (1H, dd, $J = 8.4, 2.4$ Hz, H-10'), 6.73 (1H, dd, $J = 8.4, 2.4$ Hz, H-11'), 7.14 (1H, dd, $J = 8.4, 2.4$ Hz, H-13'), 7.20 (1H, dd, $J = 8.4, 2.4$ Hz, H-14'), three aromatic singlet protons at δ_{H} 5.65 (1H, s, H-5), 6.45 (1H, s, H-5'), 5.63 (1H, s, H-8'), two methines at δ_{H} 3.96 (1H, br d, $J = 10.2$ Hz, H-1), 3.66 (1H, dd, $J = 11.4, 4.2$ Hz, H-1'), three singlet methoxy groups (δ_{H} 3.48, 3.60, and 3.93, each 3H), and two *N*-CH₃ groups (δ_{H} 2.15 and 2.58, s, each 3H), which were closely related to those of fangchinoline (**12**) [14], except for the significantly upfield shift of H-5 ($\Delta\delta$ 0.64). The ¹³C NMR data (Table 2) together with HSQC data showed the presence of a carbonyl carbon (δ_{C} 175.3, C-7) and an oxygenated quaternary carbon (δ_{C} 67.7, C-4a). The HMBC correlations from H-5 to C-6, C-7, C-8a, and C-4, from H-1 to C-4a, C-8, and C-8a, and from H-3 to C-4a confirmed the carbonyl and hydroxy group were located at C-7 and C-4a, respectively. Further analysis of ¹H-¹H COSY, HMBC (Fig. 2), and ROESY data, the 2D structure of **5** was established as shown. Additionally, the MS/MS spectrum exhibited a weak ion peak at m/z 398 (Fig. S53, Supporting Information), which corresponded to the upper half of compound **5**. The absolute configuration of **5** was elucidated as 1*S*, 4*aR*, 1'*S* based on the experimental and calculated ECD spectra (Fig. 5). Therefore, compound **5** was named fefangjine N.

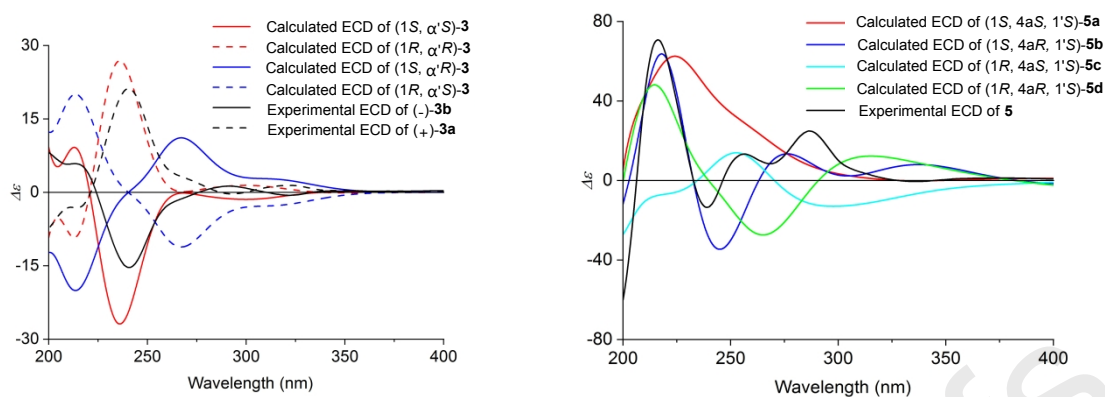


Fig. 5. Calculated and Experimental ECD spectra of compounds **3** and **5**.

Compound **6** was found to possess a molecular formula of $C_{37}H_{40}O_8N_2$ as deduced from the HRESIMS ion at m/z 641.2858 $[M+H]^+$ (calcd for $C_{37}H_{41}O_8N_2$, 641.2857). From comparing the 1D NMR data (Tables 3 and 4) of **6** with those of **5**, the most significant differences resided in the 2'-*N*-CH₃ (δ_H 3.34, δ_C 56.5), a methine (δ_H 4.38, H-1'; δ_C 77.9, C-1'), and a methylene (δ_H 3.96, 3.67, H-3'; δ_C 59.4, C-3'), which were more downfield than those of **5** (respectively at 2.58, 42.6; 3.66, 64.3; and 3.29, 2.81, 45.5). These data indicated compound **6** was a 2'-*N*-oxide of **5**. The HMBC correlations from 2'-*N*-CH₃ (δ_H 3.34) to C-1' and C-3', from H-3' to C-1', C-4a', and 2'-*N*-CH₃ (δ_C 56.5), and from H-8' to C-1' confirmed the 2'-*N*-CH₃, methine and methylene were located at N-2', C-1' and C-3' positions, respectively. The 2'-*N*-CH₃ of fangchinoline 2'-*N*- α -oxide (fenfangjine B) [8] and fangchinoline 2'-*N*- β -oxide (fenfangjine C) [8] showed at δ_H 3.34 and 2.94, respectively, which indicated that 2'-*N*-oxygen of **6** was α -oriented. In the MS/MS data of **6** (Fig. S64, Supporting Information), an ion peak at m/z 624 $[M - 16]^+$ was observed due to the loss of oxygen and a weak ion peak at m/z 398 corresponded to the upper half of molecule that lost oxygen. The absolute configuration of **6** was assigned as 1*S*, 4*aR*, 1'*S* which

is the same as that of **5**, based on the same ECD curve to those of **5** (Fig. S50 and S61 Supporting Information) and positive optical rotation value ($[\alpha]_{\text{D}}^{20} +244$ (c 0.44, CH₃Cl)). Hence, the structure of **6** was established as fenfangjine O.

Compound **7** was obtained as a white amorphous powder and its molecular formula was established as C₃₇H₄₀O₇N₂ from its HRESIMS peak at m/z 625.2907 [M+H]⁺ (calcd for C₃₇H₄₁O₇N₂, 625.2908). The ¹H and ¹³C NMR data (Tables 3 and 4) of **7** resembled those of fangchinoline (**12**) [13,14], except for a 2-*N*-CH₃, methylene of C-3, and methine of C-1 signals. The 2-*N*-CH₃ of fangchinoline (**12**) showed at δ_{H} 2.33, while that of **7** shifted to lower field and displayed at δ_{H} 2.93. The chemical shifts of C-1, 2-*N*-CH₃, and C-3 were also downfield shifted to δ_{C} 74.9, 59.8, and 57.1, respectively, comparing to the corresponding signals of fangchinoline (**12**) (δ_{C} 61.8, 42.6 and 45.3). These features suggested that **7** was a 2-*N*-oxide of fangchinoline. The 2-*N*-CH₃ of tetrandrine 2-*N*- β -oxide (fenfangjine A) [8], tetrandrine 2-*N*- β , 2'-*N*- β -dioxide [16], and tetrandrine 2-*N*- β , 2'-*N*- α -dioxide [16] displayed at δ_{H} 3.08, 3.06, and 3.06, respectively, indicating **7** was a fangchinoline-2 β -*N*-oxide. In addition, the ROESY correlation of 2-*N*-CH₃ with H-14 confirmed that the 2-*N*-oxygen was β -oriented (Fig. 3). In the MS/MS data of **7** (Fig. S75, Supporting Information), an ion peak at m/z 381 was observed because of the upper half of molecule losing one oxygen and proton. The positive optical rotation value of **7** ($[\alpha]_{\text{D}}^{20} +222$ (c 1.0, CH₃Cl)) and its similar ECD spectrum to that of fangchinoline (**12**) (Fig. S72 and S115, Supporting Information) indicated that **7** possessed the same 1*S*, 1'*S* configurations as fangchinoline (**12**). Finally, the absolute

configuration of **7** was confirmed by the reduction (Fig. 6) of **7** with zinc powder and HCl yielding fangchinoline (**12**) whose absolute configuration was confirmed by single-crystal X-ray diffraction analysis [Flack parameter 0.10 (15)] (Fig. 4). Therefore, compound **7** was elucidated as fangchinoline-2 β -*N*-oxide and named fenfangjine P.

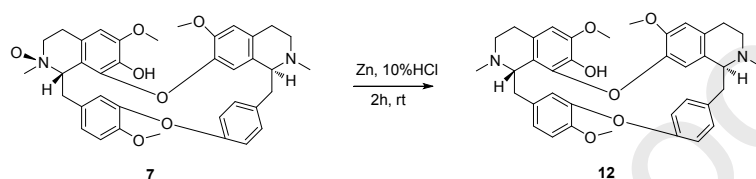


Fig. 6. Reduction of compound **7**.

Compound **8** was isolated as a white amorphous powder and assigned a molecular formula of $C_{37}H_{40}O_8N_2$ based on the HRESIMS peak at m/z 641.2858 $[M+H]^+$ (calcd for $C_{37}H_{41}O_8N_2$, 641.2857). The 1D NMR features (Tables 3 and 4) of **8** were similar to those of **7**, except that the 2'-*N*- CH_3 signal was observed at δ_H 2.87 in **8**. This implied compound **8** was a 2-*N*, 2'-*N*-dioxide of fangchinoline. The ROESY correlation of 2'-*N*- CH_3 with H-1' revealed that the 2'-*N*- CH_3 was on the same side as the H-1'. The MS/MS data of compound **8** displaying a fragment ion peak at m/z 414 (Fig. S86, Supporting Information) corresponded to the upper half of the molecule. The absolute configurations of C-1 and C-1' were assigned as 1*S*, 1'*S* based on the positive optical rotation value of **8** ($[\alpha]_D^{20} +298$ (c 0.57, CH_3Cl)) and its similar ECD spectrum (Fig. S83 and S72, Supporting Information) to that of **7**. In addition, the reduction of **8** with zinc powder and HCl afforded fangchinoline (**12**). Thus, the

structure of **8** was confirmed as fangchinoline-2 β -N, 2' β -N-dioxide and named fenfangjine Q.

Compound **9**, a white amorphous powder, had the same molecular formula, C₃₇H₄₀O₈N₂, as **8** according to the HRESIMS peak at m/z 641.2856 [M+H]⁺ (calcd for C₃₇H₄₁O₈N₂, 641.2857). The ¹H and ¹³C NMR resonances (Tables 3 and 4) of **9** were very close to those of **8**. The obvious difference involved the chemical shift of 2'-N-CH₃, implying the oxygen orientation was different at the 2'-N position. In the ¹H NMR spectrum, the 2'-N-CH₃ signal of **8** showed at δ_H 2.88, while that of **9** was downfield shifted by 0.62 ppm and showed at δ_H 3.49, which suggested compound **9** was a fangchinoline-2 β -N, 2' α -N-dioxide [8]. The MS/MS data of compound **9** exhibited an ion peak at m/z 398 (Fig. S97, Supporting Information) due to the upper half of the molecule losing one oxygen. The ECD spectra of **8** and **9** (Fig. S83 and S94, Supporting Information) were very similar, and the reduction of **9** with zinc powder and HCl yielded fangchinoline (**12**), which indicated compound **9** also possessed the 1*S*,1'*S* configurations. Therefore, the structure of fangchinoline-2 β -N, 2' α -N-dioxide (**9**) was deduced as shown and named fenfangjine R.

Compound **10** was obtained as a white amorphous powder and was determined to have same molecular formula, C₃₇H₄₀O₇N₂, as **7** from the HRESIMS data (m/z 625.2910 [M+H]⁺, calcd for C₃₇H₄₁O₇N₂, 625.2908). The NMR data (Tables 3 and 4) of **10** were similar to those of **7**, except for the chemical shift of one methoxy group. The location of methoxy group (δ_H 3.12) was confirmed by the HMBC correlation of OCH₃-7 (δ_H 3.12) with C-7. In the MS/MS spectrum, a weak fragment ion peak at m/z

396 (Fig. S108, Supporting Information) was observed, indicating the upper half of compound **10** lost the oxygen. In the ROESY spectrum of **10**, the correlations of 2-*N*-CH₃ (δ_{H} 3.01) with H-14 confirmed the 2-*N*-oxygen was β -oriented. The positive optical rotation value of **10** ($[\alpha]_{\text{D}}^{20} +268$ (c 0.1, CHCl₃)) and its similar ECD curve to that of **7** (Fig. S105 and S72, Supporting Information) indicated **10** possessed the same 1*S*,1'*S* configurations as **7**. Consequently, the structure of **10** was established and named fenfangjine S.

The anti-inflammatory activities of compounds **1-18** were tested by inhibiting against NO generation induced by LPS in murine peritoneal macrophage cells. Dexamethasone (DXM) was used as a positive control. Compounds **1-4** and **14-16** inhibited NO production with 51.94 to 73.31% inhibition at the concentration of 10 μM (Table 5). Other compounds inhibited NO production with inhibitory rates of < 50%. Compounds **1**, **15**, and **16** showed the better anti-inflammatory activities with IC₅₀ values of 15.26 ± 2.99 , 6.12 ± 0.25 , and 5.92 ± 1.89 μM , respectively. Based on a preliminary structure-activity relationship analysis, the OCH₃-7 and OCH₃-12 might be the activating groups. Compounds (**1-18**) were also evaluated for their cytotoxic activities against for five human cancer cells (A549, CMF-7, HCT-116, HepG2, and Capan 2). Only compound **18** exhibited cytotoxic activities against MCF-7, HCT-116, and HepG2 cell lines with IC₅₀ values of 2.81 ± 0.06 , 3.66 ± 0.26 , and 2.85 ± 0.15 μM , respectively. Other compounds were inactive (IC₅₀ > 10 μM). (positive control taxol, IC₅₀ < 0.01 μM).

In summary, a total of 18 bisbenzylisoquinoline alkaloids, including ten new bisbenzylisoquinoline alkaloids (**1-10**) and eight known compounds (**11-18**), were obtained from the roots of *Stephania tetrandra*. The absolute configurations of compounds **1**, **2**, and **12** were unambiguously determined by X-ray crystallography. The reductions of compounds **7-9** only yielded compound **12**, which revealed the absolute configurations of C-1 and C-1' of **7-9** were same as the those of **12**. Compound **3**, constituted from a pair of bisbenzylisoquinoline enantiomers, was a partial racemate and was discovered by chiral HPLC. This case indicated that it is necessary to increase attention to the partial racemates from natural products, which are inadvertently regarded as optically pure chemical entities. Among these isolated compounds, compounds **1-4** and **14-16** showed anti-inflammatory activities and compound **18** possessed cytotoxicity.

Notes

The authors declare no competing financial interests.

Acknowledgments

This work was financially supported by Chinese Academy of Medical Sciences (CAMS) Initiative for Innovative Medicine [CAMS-12M-1-010], the State Key Laboratory of Bioactive Substance and Function of Natural Medicines [No. GTZA201803], and the Drug Innovation Major Project [2018ZX09711001-008-009].

Appendix A. Supplementary material

The material (1D and 2D NMR, UV, IR, CD, and HRESIMS/MS data for compounds **1-10**) is provided in the Supporting Information.

REFERENCES

- [1] K.P. Guha, B. Mukherjee, R. Mukherjee, *J. Nat. Prod.* 42 (1979) 1-84.
- [2] C. Weber, T. Opatz, *Alkaloids Chem. Biol.* 81 (2019) 1-114.
- [3] C.K. Angerhofer, H. Guinaudeau, V. Wongpanich, J.M. Pezzuto, G.A. Cordell, *J. Nat. Prod.* 62 (1999) 59-66.
- [4] Y. Kondo, F. Takano, H. Hojo, *Biochem. Pharmacol.* 46 (1993) 1887-1892.
- [5] A.L. Otshudi, S. Apers, L. Pieters, M. Claeys, C. Pannecouque, E. De Clercq, A. Van Zeebroeck, S. Lauwers, M. Frederich, A. Foriers, *J. Ethnopharmacol.* 102 (2005) 89-94.
- [6] A. Zahari, A. Ablat, Y. Sivasothy, J. Mohamad, M.I. Choudhary, K. Awang, *Asian Pac. J. Trop. Med.* 9 (2016) 328-332.

- [7] National Pharmacopoeia Committee, Pharmacopoeia of Peoples Republic of China. Part 1, Chemical Industry Press, Beijing, 2015, pp. 148-149.
- [8] T. Ogino, T. Sato, H. Sasaki, M. Chin, H. Mitsuhashi, *Heterocycles* 27 (1988) 1149-1154.
- [9] J.Z. Deng, S.X. Zhao, F.C. Lou, *J. Nat. Prod.* 53 (1990) 993-994.
- [10] J.Z. Deng, S.X. Zhao, T. Lu, F.C. Lou, *Chin. Chem. Lett.* 2 (1991) 231-232.
- [11] N. Bhagya, K.R. Chandrashekar, *Phytochemistry* 125 (2016) 5-13.
- [12] L.Z. Lin, H.L. Shieh, C.K. Angerhofer, J.M. Pezzuto, G.A. Cordell, *J. Nat. Prod.* 56 (1993) 22-29.
- [13] J. Stanstrup, J.S. Schmidt, H.B. Rasmussen, P. Mølgaard, A. Guzmán, D. Staerk, *Biochem. Syst. Ecol.* 38 (2010) 450-453.
- [14] S.A. Philipov, R.S. Istatkova, *Phytochemistry* 44 (1997) 1591-1594.
- [15] K. Dahmen, P. Pachaly, F. Zymalkowski, *Arch. Pharm.* 310 (1977) 95-102.
- [16] M.B. Lin, W. Zhang, X.W. Zhao, J.X. Lu, *Acta Chim. Sinica* 42 (1984) 199-204.
- [17] X. Zeng, Y. Dong, G. Sheng, X. Dong, X. Sun, J. Fu, *J. Ethnopharmacol.* 108 (2006) 317-319.
- [18] H. Guinaudeau, L.Z. Lin, N. Ruangrunsi, G.A. Cordell, *J. Nat. Prod.* 56 (1993) 1989-1992.
- [19] S.M. Kupchan, A.J. Liepa, R.L. Baxter, H.P.J. Hintz, *J. org. Chem.* 38 (1973) 1846-1852.
- [20] J. Baldas, I.R.C. Bick, T. Ibuka, R.S. Kapil, Q.N. Porter, *J. Chem. Soc., Perkin Trans. 1* (1972) 592-596.
- [21] W.N. Wu, M.D. Moyer, *J. Pharm. Biomed. Anal.* 34 (2004) 53-66.

[22] S.F. Hussain, L. Khan, H. Guinaudeau, J.E. Leet, A.J. Freyer, M. Shamma,
Tetrahedron 40 (1984) 2513-2517.

Table 1 ¹H NMR Data for Compounds **1-5** in CDCl₃

position	1^a	2^b	3^a	4^a	5^a
1	3.75 brd (9.0)	3.74 dd (11.2, 2.4)	4.11 brs		3.96 brd (10.2)
2- <i>N</i> -CH ₃	2.32 s	2.26 s	2.50 s		2.15 s
3	3.47 m	3.55 m	2.90 brs	3.92 m	3.45 m
	2.89 m	2.59-2.67 overlap	2.41 brs	3.62 m	2.52-2.58 overlap
4	2.90 m	2.98 m	2.32 brs	2.63 m	1.90 m
	2.41 m	2.59-2.67 overlap	1.72 brs		
5	6.35 s	6.74 s	6.47 s	6.44 s	5.65 s
α	2.68 dd (13.8, 10.2)	2.76-2.87 overlap	2.73 dd (13.8, 3.6)		3.18 dd (14.4, 10.2)
	2.61 brd (13.8)		2.06 brs		2.52-2.58 overlap
10	6.47 d (1.8)	6.28 d (1.6)	6.69-6.74 overlap	6.93 d (1.8)	6.68 d (1.8)
13	6.86 d (8.4)	6.88 d (8.4)	6.69-6.74 overlap	6.92 d (8.4)	6.87 d (8.4)
14	6.89 dd (8.4, 1.8)	6.95 dd (8.4, 1.6)	6.75 dd (7.8, 1.8)	7.46 dd (8.4, 1.2)	6.84 dd (8.4, 1.8)
15		5.10 d (9.2)			
		4.73 d (9.2)			
1'	4.74 dd (7.2, 5.4)	3.82 overlap		3.67 dd (9.6, 6.0)	3.66 dd (11.4, 4.2)
2'- <i>N</i> -CH ₃	3.29 s	2.62 s		2.46 s	2.58 s
3'		3.06 m	8.37 d (5.4)	3.38 m	3.29 m
		2.54 m		2.77-2.81 overlap	2.81 m
4'		2.76-2.87 overlap	7.50 d (5.4)	2.87 m	2.90 m

		2.44 brd (15.2)		2.71 m	2.60 m
5'	7.21 s	6.49 s	7.10 s	6.54 s	6.44 s
8'	6.40 s	6.48 s	7.09 s	5.52 s	5.63 s
α'	3.51 m	3.33 brd (14.0)	6.08 s	3.21 dd (12.6, 5.4)	3.25 dd (12.6, 4.2)
	2.97 dd (14.4, 4.4)	2.76-2.87 overlap		2.77-2.81 overlap	2.52-2.58 overlap
10'	6.50 dd (8.4, 2.4)	7.10 brs	6.69-6.74 overlap	6.36 dd (8.4, 1.8)	6.33 dd (8.4, 2.4)
11'	6.79 dd (8.4, 2.4)	6.70 brd (8.4)	6.68 dd (8.4, 1.8)	6.62 dd (8.4, 1.8)	6.73 dd (8.4, 2.4)
13'	7.09 dd (8.4, 2.4)	6.70 brd (8.4)	6.69-6.74 overlap	7.13 dd (8.4, 2.4)	7.14 dd (8.4, 2.4)
14'	7.29 dd (8.4, 2.4)	7.10 brs	7.71 dd (7.8, 1.8)	7.24 dd (8.4, 1.8)	7.20 dd (8.4, 2.4)
6-OCH ₃	3.78 s	3.88 s	3.97 s	3.78 s	3.60 s
7-OCH ₃	3.23 s	3.82 s	3.56 s	2.98 s	
12-OCH ₃	3.92 s	3.88 s	3.89 s	3.96 s	3.93 s
6'-OCH ₃	3.48 s		3.94 s	3.64 s	3.48 s

^aRecorded at 600 MHz. ^bRecorded at 400 MHz (50°C).

Table 2 ¹³C NMR (150 MHz) Data for Compounds **1-5** in CDCl₃

position	1	2	3	4	5
1	61.6, CH	61.7, CH	59.2, CH	165.1, C	63.2, CH
2- <i>N</i> -CH ₃	42.5, CH ₃	42.6, CH ₃	43.5, CH ₃		43.3, CH ₃
3	44.3, CH ₂	43.7, CH ₂	48.8, CH ₂	47.5, CH ₂	44.9, CH ₂
4	22.3, CH ₂	23.5, CH ₂	27.6, CH ₂	26.7, CH ₂	35.7, CH ₂
4a	128.9, C	130.4, C	133.7, C	134.9, C	67.7, C
5	106.8, CH	113.9, CH	107.9, CH	105.7, CH	118.4, CH
6	151.3, C	151.1, C	151.6, C	156.9, C	149.2, C
7	138.2, C	147.7, C	139.3, C	138.1, C	175.3, C
8	147.9, C	127.4, C	144.5, C	149.6, C	143.6, C
8a	122.9, C	130.5, C	122.7, C	113.7, C	137.0, C
α	41.6, CH ₂	42.1, CH ₂	40.1, CH ₂	193.3, C	39.4, CH ₂
9	134.9, C	132.6, C	131.5, C	130.9, C	134.75, C
10	116.6, CH	118.2, CH	116.9, CH	121.3, CH	115.7, CH
11	148.8, C	146.9, C	149.2, C	149.4, C	149.0, C
12	147.5, C	148.8, C	146.5, C	153.7, C	147.8, C
13	111.9, CH	112.3, CH	110.7, CH	111.5, CH	111.9, CH
14	123.5, CH	125.1, CH	124.2, CH	124.0, CH	123.3, CH
15		62.1, CH ₂			
1'	61.2, CH	64.9, CH	157.4, C	64.1, CH	64.3, CH

2'-N-CH ₃	27.8, CH ₃	44.1, CH ₃		42.7, CH ₃	42.6, CH ₃
3'		51.8, CH ₂	138.4, CH	45.3, CH ₂	45.5, CH ₂
4'	168.6, C	29.4, CH ₂	120.0, CH	24.9, CH ₂	25.1, CH ₂
4a'	127.7, C	127.7, C	134.5, C	130.1, C	127.4, C
5'	106.7, CH	110.5, CH	105.8, CH	113.4, CH	112.7, CH
6'	150.8, C	143.4, C	152.8, C	150.8, C	146.4, C
7'	149.0, C	143.1, C	145.3, C	145.0, C	141.5, C
8'	115.5, CH	113.4, CH	109.7, CH	120.9, CH	119.2, CH
8a'	137.0, C	129.8, C	120.8, C	128.2, C	128.8, C
α'	37.2, CH ₂	38.7, C	72.8, CH	38.4, CH ₂	39.7, CH ₂
9'	133.0, C	133.8, C	140.9, C	135.0, C	134.79, C
10'	131.1, CH	131.4, CH	130.1, CH	132.5, CH	132.5, CH
11'	122.1, CH	117.7, CH	124.3, CH	122.5, CH	120.1, CH
12'	154.9, C	155.0, C	154.8, C	157.0, C	154.1, C
13'	121.5, CH	117.7, CH	123.5, CH	121.5, CH	121.7, CH
14'	130.3, CH	131.4, CH	131.0, CH	129.8, CH	130.5, CH
6-OCH ₃	55.97, CH ₃	55.8, CH ₃	56.05, CH ₃	56.1, CH ₃	55.2, CH ₃
7-OCH ₃	60.4, CH ₃	61.9, CH ₃	60.6, CH ₃	60.0, CH ₃	
12-OCH ₃	56.3, CH ₃	56.3, CH ₃	56.15, CH ₃	56.3, CH ₃	56.3, CH ₃
6'-OCH ₃	56.03, CH ₃		56.11, CH ₃	56.8, CH ₃	55.7, CH ₃

Table 3 ¹H NMR (600 MHz) Data for Compounds 6-10

position	6 ^a	7 ^a	8 ^a	9 ^b	10 ^b
1	3.91 m	4.87 brd (10.2)	4.97 brd (10.2)	4.75 brd (10.2)	4.77 brd (9.6)
2-N-CH ₃	2.21 s	2.93 s	3.05 s	2.95 s	3.01 s
3	3.47 m	3.78 m	3.84 m	3.44 m	4.07 m
	2.59 m	3.42 m	3.63 m	3.32 m	3.33 m
4	2.03 m	3.56 m	3.63 m	3.37 overlap	3.41 m
	1.91 m	2.71-2.76 overlap	2.74 m	2.83 overlap	3.04 m
5	5.75 s	6.34 s	6.40 s	6.46 s	6.54 s
α	3.20 m	3.10 brd (16.8)	3.25 brd (16.8)	2.98 brd (16.8)	2.84-2.94 overlap
	2.60 m	2.61 overlap	2.71 m	2.87 m	
10	6.66 d (1.8)	6.73 s	6.79 d (1.8)	6.75 d (1.8)	6.76 d (1.8)
13	6.87 overlap	6.82 d (8,4)	6.88 d (7.8)	7.00 d (7.8)	6.84 d (8.4)
14	6.87 overlap	6.67 dd (8.4, 2.4)	6.69 dd (7.8, 1.8)	6.91 dd (7.8, 1.8)	6.80 dd (8.4, 1.8)
1'	4.37 brs	3.88 m	4.63 dd (12.0, 4.8)	4.50 dd (12.0, 6.0)	4.00, dd (11.4, 6)
2'-N-CH ₃	3.34 s	2.61 s	2.87 s	3.49 s	2.62 s
3'	3.96 m	3.34 m	3.95 m	4.14 m	3.46 m
	3.67 m	2.85 m	3.38 m	4.03 m	2.93 overlap
4'	3.18 m	2.91 m	3.17 dd (18.0, 7.2)	3.37 overlap	2.84-2.94 overlap
	3.10 m	2.71-2.76 overlap	2.95 m	3.03 dd (17.4, 6.6)	
5'	6.54 s	6.48 s	6.54 s	6.70 s	6.67 s

8'	5.71 s	5.94 s	6.04 s	5.95 s	5.97 s
α'	4.35 brs	3.23 dd (12.6, 5.4)	3.77 m	3.66 dd (12.0, 6.0)	3.29 dd (12.6, 6.0)
	2.49 t (12.6)	2.71-2.76 overlap	2.46 t (12.0)	2.83 overlap	2.85 overlap
10'	6.30 dd (8.4, 2.4)	6.42 dd (8.4, 2.4)	6.34 dd (8.4, 1.8)	6.43 dd (8.4, 2.4)	6.42 dd (8.4, 2.4)
11'	6.78 dd (8.4, 2.4)	6.89 dd (8.4, 2.4)	6.83 dd (8.4, 2.4)	6.86 dd (8.4, 2.4)	6.87 dd (8.4, 2.4)
13'	7.18 dd (8.4, 2.4)	6.97 dd (8.4, 2.4)	6.11 brs	6.96 dd (8.4, 2.4)	6.98 dd (8.4, 2.4)
14'	7.50 dd (8.4, 2.4)	7.31 dd (8.4, 2.4)	7.25 brs	7.49 dd (8.4, 2.4)	7.43 dd (8.4, 2.4)
6-OCH ₃	3.63 s	3.75 s	3.79 s	3.76 s	3.77 s
7-OCH ₃					3.12 s
12-OCH ₃	3.92 s	3.94 s	3.90 s	3.92 s	
6'-OCH ₃	3.55 s	3.38 s	3.43 s	3.41 s	3.45 s

^ameasured in CDCl₃. ^bmeasured in CD₃OD.

Table 4 ¹³C NMR (150 MHz) Data for Compounds **6-10**

position	6^a	7^a	8^a	9^b	10^b
1	63.8, CH	74.9, CH	74.68, CH	77.1, CH	77.2, CH
2- <i>N</i> -CH ₃	43.4, CH ₃	59.8, CH ₃	60.1, CH ₃	60.3, CH ₃	60.7, CH ₃
3	45.5, CH ₂	57.1, CH ₂	57.5, CH ₂	58.39, CH ₂	58.3, CH ₂
4	36.1, CH ₂	24.7, CH ₂	24.6, CH ₂	25.2, CH ₂	25.5, CH ₂
4a	67.9, C	121.2, C	118.6, C	120.6, C	126.1, C
5	118.5, CH	104.6, CH	105.3, CH	106.2, CH	106.9, CH
6	149.1, C	146.8, C	150.2, C	149.4, C	153.7, C
7	175.3, C	135.5, C	137.4, C	137.1, C	139.6, C
8	143.0, C	141.1, C	143.4, C	143.2, C	148.6, C
8a	138.1, C	119.7, C	120.8, C	121.6, C	121.5, C
α	40.0, CH ₂	43.3, CH ₂	44.0, CH ₂	43.3, CH ₂	43.3, CH ₂
9	134.7, C	131.9, C	132.1, C	133.6, C	132.2, C
10	116.1, CH	115.0, CH	114.0, CH	115.8, CH	116.0, CH
11	148.8, C	150.4, C	150.0, C	151.4, C	150.2, C
12	148.1, C	148.3, C	148.2, C	149.6, C	147.1, C
13	112.1, CH	111.5, CH	112.7, CH	113.6, CH	117.0, CH
14	123.7, CH	122.8, CH	123.2, CH	124.8, CH	124.9, CH
1'	77.9, CH	63.7, CH	74.71, CH	78.3, CH	64.4, CH
2'- <i>N</i> -CH ₃	56.5, CH ₃	42.8, CH ₃	54.5, CH ₃	58.43, CH ₃	42.4, CH ₃

3'	59.4, CH ₂	45.4, CH ₂	58.5, CH ₂	58.4, CH ₂	45.6, CH ₂
4'	26.8, CH ₂	25.9, CH ₂	26.2, CH ₂	25.3, CH ₂	26.0, CH ₂
4a'	122.4, C	128.54, C	122.0, C	126.3, C	129.6, C
5'	112.2, CH	113.3, CH	113.0, CH	113.1, CH	113.3, CH
6'	148.8, C	149.1, C	151.0, C	151.2, C	150.4, C
7'	143.0, C	143.3, C	146.2, C	145.4, C	144.9, C
8'	119.4, CH	120.1, CH	118.6, CH	122.2, CH	121.4, CH
8a'	125.4, C	128.50, C	123.32, C	124.7, C	128.6, C
α'	38.5, CH ₂	37.3, CH ₂	38.1, CH ₂	40.9, CH ₂	37.5, CH ₂
9'	132.4, C	136.0, C	133.4, C	134.1, C	136.8, C
10'	132.9, CH	132.3, CH	132.3, CH	133.5, CH	133.3, CH
11'	120.4, CH	122.5, CH	123.27, CH	123.3, CH	122.9, CH
12'	155.0, C	153.3, C	153.7, C	155.7, C	155.3, C
13'	122.0, CH	121.7, CH	121.6, CH	122.8, CH	122.5, CH
14'	131.0, CH	130.7, CH	130.5, CH	132.4, CH	132.1, CH
6-OCH ₃	55.4, CH ₃	56.4, CH ₃	56.5, CH ₃	56.2, CH ₃	56.4, CH ₃
7-OCH ₃					60.3, CH ₃
12-OCH ₃	56.3, CH ₃	56.2, CH ₃	56.3, CH ₃	56.7, CH ₃	
6'-OCH ₃	55.8, CH ₃	56.5, CH ₃	56.2, CH ₃	56.2, CH ₃	55.9, CH ₃

^ameasured in CDCl₃. ^bmeasured in CD₃OD.

Table 5 Anti-inflammatory activities of compounds **1-4** and **14-16**

compound ^a	inhibition rate (%)
1	70.23
2	63.69
3a	51.94
3b	56.62
4	55.84
14	55.84
15	73.31
16	71.60
DXM^b	94.88

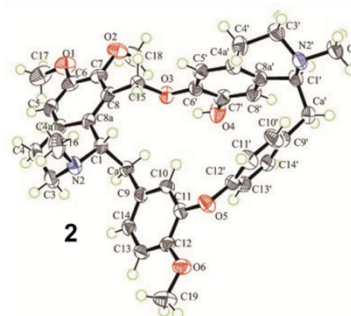
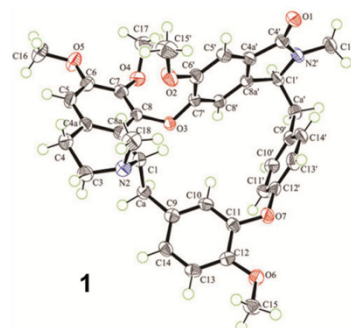
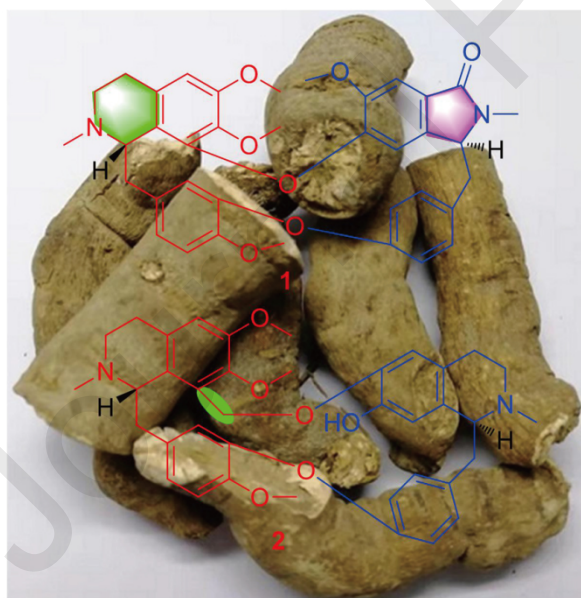
^aInhibiting NO production at the concentration of 10 μM.

^bPositive control.

Declaration of interests

The authors declare that they have no known competing financial interests or personal relationships that could have appeared to influence the work reported in this paper.

The authors declare the following financial interests/personal relationships which may be considered as potential competing interests:

**Highlights**

- Ten new compounds were isolated from the roots of *Stephania tetrandra*.
- Compounds **1**, **2**, and **12** were unambiguously determined by X-ray crystallography.
- Compound **3** was a partial racemate and was discovered by chiral HPLC.
- Compounds **1-4** and **14-16** showed anti-inflammatory activities